GEOPHYSICAL RESEARCH LETTERS, VOL. 21, NO. 18, PAGES 1951-1954, SEPTEMBER 1, 1994

Some effects of anisotropy on velocity contrasts between subducting lithosphere and overriding mantle

Tom Shoberg and Craig R. Bina
Department of Geological Sciences, Northwestern University, Evanston, IL

Abstract. We compute velocity anisotropy for three models of preferred crystal alignment due to finite strain in the mantle which, when juxtaposed with computed anisotropy in subducted lithosphere and neglecting other effects, give velocity contrasts that we compare with those observed. We find a strong dip dependence for computed velocity contrasts due to slow axis alignment in the overriding mantle perpendicular to the slab-mantle interface. Moreover, for an isotropic mantle wedge or convergence-parallel flow, it is difficult to produce greater velocity in the subducting slab than the overlying mantle for near-vertical propagation even with high strain rates. We do, however, obtain positive contrasts using a dip axis-parallel flow model, which is the only one that yields contrasts that approach observations from the Japan Trench.

Introduction

Velocity contrasts between subducting slabs and overlying mantle give rise to measurable travel time anomalies, relative to reference velocity models, for seismic phases crossing the slab-mantle interface. Many studies report travel time anomalies that appear too large to be due to slab-mantle temperature contrasts alone. We consider the extent to which such "excess" anomaly (2-6%) may be attributable to seismic anisotropy. Such velocity contrasts are important because they provide constraints on the geometry of subducting slabs through velocity structure studies. Furthermore, amplitude and travel time anomalies induced by such velocity contrasts, when combined with a velocity-temperature relation, help to constrain thermal models of subducting slabs [*Helffrich et al.*, 1989].

Several studies have used ScSp arrivals and converted-P arrivals (S-waves that are "guided" up the subducting slab and converted to P-waves upon refraction into the overlying mantle) to determine velocity contrasts between subducting lithosphere and overlying mantle. ScSp arrivals are nearly vertically incident and are converted from S to P at this interface. Converted-P arrivals are "guided" through a low velocity channel, often assumed to be largely isotropic oceanic crust, surrounded by high velocity overlying mantle and the higher velocity upper mantle of the subducting lithosphere. Results from these studies suggest a velocity contrast between subducting lithosphere and overlying mantle of between 4 and 12%, limited in depth extent from 30 km to 350 km [e.g., *Fukao et al.*, 1978, 1983; *Matsuzawa et al.*, 1986; *Nakanishi et al.*, 1981; *Snoke et al.*, 1977]. Recently *Helffrich et al.* [1989] considered several possible mechanisms for generating such observations. While their preferred mechanism combines thermal contrasts, chemical discontinuities, and deflection of the α-β olivine phase boundary, they also suggested that olivine crystal orientation might be partially responsible. We test this latter mechanism using models of lattice preferred orientations in subducting slabs and idealized flow patterns in the overlying mantle. From the juxtaposition of slab and mantle crystal orientations, we calculate theoretical velocity contrasts.

We assume a lattice preferred orientation in the upper lithosphere that becomes "frozen" in as it cools, thereafter remaining constant, in the local coordinate system, even if the local stress field changes. We also assume, following previous experimental, field, and theoretical considerations, that the fast axes of olivine crystals tend to align with the axis of greatest finite strain during induced mantle flow at spreading centers [e.g., *Hess*, 1964; *Raitt et al.*, 1971; *McKenzie*, 1979; *Ribe*, 1989a]. Such alignment suggests that olivine fast axes in the ocean floor roughly parallel the paleospreading direction, an assumption which appears to be consistent with seismic observations [e.g., *Forsyth*, 1975; *Shearer and Orcutt*, 1986; *Nishimura and Forsyth*, 1989]. Crystal axis orientations in subducting slabs are computed by mapping these surface orientations down-dip through a rotation about the dip axis.

McKenzie [1979] suggested that lattice preferred orientation in the mantle wedge overlying the slab would be induced through viscous shearing of the mantle by the subducting lithosphere, giving rise to strong anisotropy in the overlying mantle. *Ribe* [1989a; 1989b] and *Ribe and Yu* [1991] confirmed and extended this idea using a plastic deformation model with monomineralic polycrystals. We investigate three models for flow-induced anisotropy of the overlying mantle: random orientation (or isotropic, Model I), fast axis aligned with convergence direction (Model CD) [*McKenzie*, 1979], and fast axis aligned with slab dip axis (Model DA). Model I might result from high water content in the mantle wedge arising from dehydration reactions in the subducting slab. Such hydration might allow strain to be taken up largely by diffusion creep, yielding more isotropic crystal orientations [*Karato*, 1992]. Model CD might arise due to finite strains induced through viscous shearing of the overlying mantle by the subduction of stronger lithosphere [e.g., *McKenzie*, 1979; *Ribe*, 1989a]. Such strains would yield a fast axis parallel to the projection of the surface convergence vector onto the slab-mantle interface. Model DA derives from the proposed retrograde motion of lithospheric slabs away from the overriding plate, inducing trench-parallel flow in the underlying mantle [*Russo and Silver*, 1994] which, in turn, may induce trench-parallel counterflow in the overlying mantle. Such an alignment might help explain shear-wave splitting observations of *Ando et al.* [1983] north of Honshu (though not their southern data). *Fischer and Yang* [1994] report shear-wave splitting consistent with Model CD at the Kuril-Kamchatka trench but also find trench-parallel polarizations in the northern extreme of their study area.

Our models generate velocity contrasts that are largely controlled by the dip of the subducting lithosphere for near-vertical

Paper number 94GL01613
0094-8534/94/94GL-01613$03.00

propagation paths, such as those for ScS and ScSp arrivals. There is a lesser but significant dip effect on rays traveling up-dip in the slab and then vertically in the mantle (e.g., converted-P phases). For moderate strain rates and ideal geometries, Model CD can not explain the observed velocity contrasts for near-vertical ScSp studies. Model I can do so only for steeply dipping slabs, whereas Model DA can do so even with moderate dip angles. We use these models to calculate velocity contrasts for the Japan Trench.

Method

Olivine crystals in oceanic lithosphere are assumed to have their fast axes approximately aligned with the paleospreading direction, the intermediate axis aligned horizontally perpendicular to this, and the slow axis vertically aligned. This orientation allows us to define directional cosines (n_i) for vertical propagation of compressional waves in the local crystallographic coordinate system:

$$n_1 = \sin(\psi+\phi)\sin\theta, \quad n_2 = \sin(\psi+\phi)\cos\theta, \quad n_3 = \cos(\psi+\phi).$$

where θ is the acute angle between the fast axis and the strike of the trench, ψ is the dip of the slab, and ϕ is the angle between the finite-strain-induced fast axis and the flow direction (Figure 1). ϕ is considered positive in a clockwise direction. The "guided" wave or up-dip propagation directional cosines are similar except that $\psi = 0$ for up-dip propagation.

To determine the velocity (V) of plane waves propagating through an anisotropic material, we employ these n_i values and the elastic stiffness coefficients c_{ijkl} compiled by *Estey and Douglas* [1986] in the Christoffel equation [*Musgrave*, 1970]:

$$\det|c_{ijkl}\, n_j n_l - \rho V^2 \delta_{ik}| = 0,$$

yielding the compressional wave velocity as the positive square root of the largest resultant eigenvalue divided by the density. Since temperature effects are more pronounced at seismic than at ultrasonic frequencies, stiffness coefficients measured at ultrasonic frequencies should underestimate velocity contrasts recorded by seismic studies [*Karato*, 1993].

Velocities in the overlying mantle are similarly determined, except that θ becomes the acute angle between the dip axis and the mantle flow direction for the non-isotropic models. For the crystal orientation in the overlying mantle using non-isotropic models, we follow the work of *McKenzie* [1979] and *Ribe* [1989a,b], aligning the fast axis along the axis of greatest finite strain for the relevant mantle flow lines. For Model CD, the fast axis parallels the plane of the slab-mantle interface in the direction of convergence. For Model DA, the fast axis also parallels the interface but along the strike of the subduction zone. For both of these models we assumed the shear plane to be the slab-mantle interface and the strain rate to be high enough for ϕ to be small. Thus as ϕ goes to zero, the slow axis aligns perpendicular to the shear plane. This orientation requires the intermediate axis to be parallel to the interface and perpendicular to the fast axis.

For simplicity we initially assume a pure olivine mantle. We also assume that the strike of a subduction zone parallels the surface manifestation of the oceanic trench. We further assume that the paleospreading direction recorded in the seafloor near the trench remained unchanged during the time required for the slab to descend about 400 km into the mantle. This direction is taken to be perpendicular to the near-trench seafloor magnetic anomaly lineations of *Cande et al.* [1989] and parallel to near-trench fracture zone trends of *Gahagan et al.* [1988]. The mean, weighted by the reciprocal standard deviation of each set of measurements, is used as the paleospreading direction at the trench. Relative and "absolute" (i.e., with respect to hot spots) convergence directions were derived from *DeMets et al.* [1990] and *Gripp and Gordon* [1990], respectively.

Helffrich et al. [1989] determined slab and mantle isotherms from numerical models employing an adiabatic mantle geotherm and induced corner flow in the overlying mantle wedge; dip, convergence rate, and lithospheric age parameters were appropriate to the Japan Trench, but they did not allow for shear heating along the mantle/slab interface. Their velocity contrast due to thermal effects alone is about 2%. Combining our velocity contrast calculations for the Japan Trench with the thermal effects calculated by *Helffrich et al.* [1989] gives results that can be tested for consistency with observations.

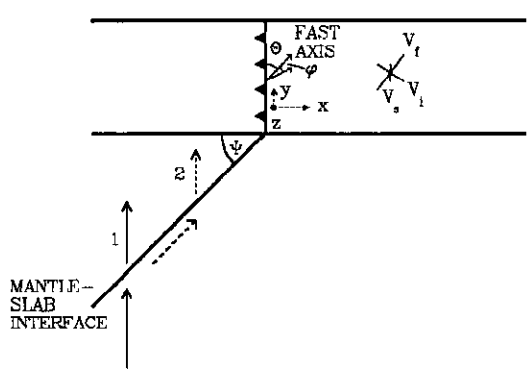

Figure 1. Cartoon of subduction zone geometry. Ray path 1 (solid line) depicts vertical propagation while 2 (dotted line) shows up-dip propagation. x, y and z refer to local coordinate system at trench. V_f, V_i, and V_s represent velocities due to crystal axis orientation, where the angle that the horizontal projection of the fast axis makes with the dip axis is denoted by Θ and the plunge by ϕ. ψ is the dip angle of the subducting slab.

Results

We consider the case in which finite strains are sufficiently high that fast axis orientations parallel idealized flow lines (ϕ=0). Figure 2 gives computed velocity contrasts between the slab and mantle for vertical ray paths (e.g., path 1 of Figure 1) through a subduction zone whose convergence direction is perpendicular to the strike of the trench. These are plotted as continuous functions of dip angle ψ for four discrete orientations θ of the fast axis in the subducting lithosphere, relative to trench strike. Greater velocities in the slab than in the mantle constitute a positive velocity contrast. Clearly, Model CD does not succeed in generating positive velocity contrasts regardless of the orientation of the crystals in the slab. Model DA, on the other hand, yields positive velocity contrasts for all orientations with $\theta > 0°$ and $\psi > 0°$, which can be quite high even at moderate dips (30-50°) for large θ. Model I yields positive velocity contrasts only at high dip angles (45-90°) with large θ. Thus, if trench-parallel flow induces fast axis alignment in the mantle wedge parallel to the dip axis of the subduction zone (DA), then slab/mantle anisotropy may contribute significantly to observed velocity contrasts. If, on the other hand, the mantle wedge is largely isotropic (I) or possesses a fast axis which parallels the convergence direction (CD), then the anisotropy contribution is opposite in sign to the observed anomalies, requiring even greater contributions from thermal effects, phase transformations, or bulk compositional contrasts.

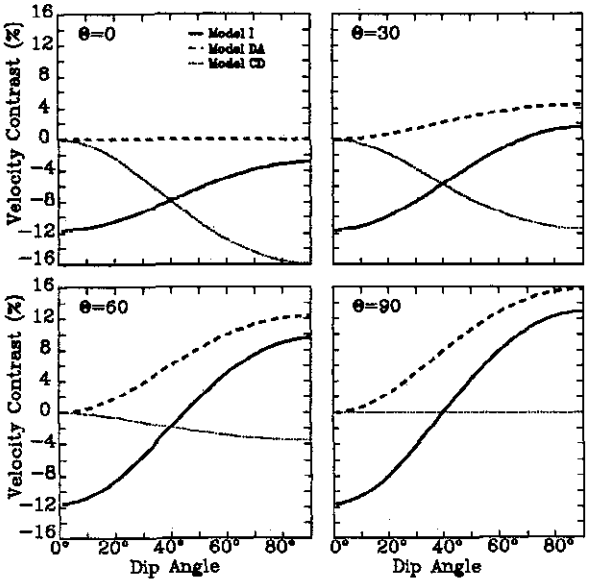

Figure 2. Velocity contrasts at slab-mantle interface ($V_{slab} - V_{mantle}$) for vertically propagating P-wave through olivine mantle and slab. Calculations do not include thermal effects. Crystal fast axes are aligned parallel to the convergence direction (CD, dotted line), parallel to the dip axis (DA, dashed line) or randomly (I, solid line). Θ is the angle between the fast axis in the slab at the surface and the dip axis.

We compare velocity contrasts from these models, combined with those due to the thermal structure of *Helffrich et al.* [1989], to seismic studies of the Japan trench by *Matsuzawa et al.* [1986] to see if anisotropy contributions might be significant. Here, the angle between the paleospreading direction and the trench azimuth gives θ for the lithosphere of 38°, and the dip of the slab is taken as 35° to be consistent with *Matsuzawa et al.* [1986]. Relative convergence directions are appropriate in the upper part of the subduction zone where lithosphere-lithosphere interaction occurs, whereas the absolute convergence directions with respect to hot spots might be appropriate for interactions between overlying mantle and subducting lithosphere. These two convergence directions are quite similar for this trench, yielding a convergence direction (θ) relative to the dip axis of 75° for Model CD. For Model DA the angle between the direction of mantle flow and the dip axis is 0°. Given these parameters and the assumption of vertical propagation through a pure olivine mantle and subducting slab, we compute velocity contrasts for vertical propagation as follows: Model I, -9%; Model CD, -3%; and Model DA, 1%. Only Model DA shows a positive contrast.

More realistic estimates can be achieved by taking a Voigt-average of mantle mineralogy. For a typical model of upper mantle composition such as the Tinaquillo Lherzolite [*Helffrich et al.*, 1989], parameters for the Japan trench yield a velocity contrast 58% of that for pure olivine, mainly due to the tendency of the orthopyroxene slow axis to align parallel to the olivine fast axis [*Peselnick and Nicholas*, 1978]. The resulting velocity contrast barely exceeds 1% for Model DA, and we assumed ideal geometries that tend to maximize velocity contrasts. Furthermore, while the incident ray in the slab may be nearly vertical, the converted-P wave traveling through the overlying mantle has a distinct non-vertical component and samples less of the slow axis in the induced mantle flow models, thereby further reducing positive velocity contrasts.

Figure 3 shows results for the "guided" wave in the slab followed by a vertical path through the mantle to a station directly up-dip from the earthquake (e.g., converted-P; path 2 of Figure 1). This geometry produces the maximum velocity contrast between the slab and the mantle for this phase. For all crystal axis orientations in the slab, we see a positive velocity contrast at low dip angles for both of the flow-induced crystal orientation mantle models. This result is not surprising as there is no dip dependence (or slow axis sampling) through the slab, but the shallower the dip, the more the slow axis will be sampled when the ray leaves the slab and travels vertically through the mantle. Model DA shows positive velocity contrasts as the fast axis in the mantle is largely unsampled. For Model CD, on the other hand, the fast axis becomes more thoroughly sampled in the overlying mantle as ψ increases, eventually yielding negative velocity contrasts. Model I gives positive velocity contrasts except when the fast axis alignment in the subducting slab nearly parallels the dip axis.

If we apply the parameters for the Japan trench, we can compute velocity contrasts for up-dip rays in each of these models (Model I, -1%; Model CD, 4%; Model DA, 9%). Again taking Voigt-averages, we see that Models I and CD give velocity contrasts much lower than those seen by *Matsuzawa et al.* [1986] for a converted S to P phase (6% compared with 2% for CD and -1% for I), but Model DA yields a 4% contrast. Again, these results are based on an ideal geometry designed to maximize velocity contrasts, although our use of ultrasonic elastic moduli will tend to underestimate these contrasts. If either model accurately represents the crystal orientation in the mantle, then the anisotropy due to olivine crystal alignment is insufficient to explain the observed velocity contrast. If Model DA accurately represents the mantle crystal orientation, then anisotropy due to olivine crystal orientation combined with thermal effects may prove significant in generating the observed velocity contrast.

Discussion

If significant velocity anisotropy persists in and around subducting slabs, then there should be a strong dip dependence to

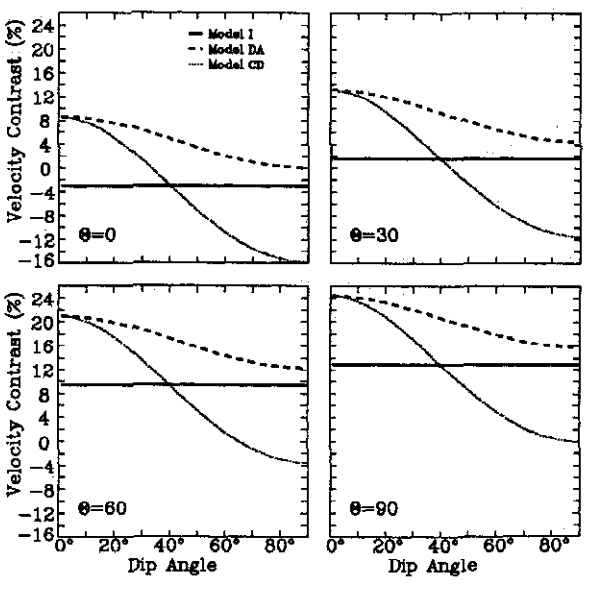

Figure 3. Velocity contrasts at slab-mantle interface for a P-wave traveling up-dip in the slab and then vertically through the overlying mantle. Otherwise consistent with Figure 2.

the effective velocity contrast sampled by each seismic phase. The dip dependence for the two phases considered here is strongest for the nearly vertical ScSp phase, as the predicted velocity contrast possesses a dip dependence in both the overlying mantle velocity and in the slab velocity. This dip dependence is due to slow axis alignment perpendicular to the slab-mantle interface; thus, larger dip angles lead to less sampling of the slow axis for near-vertical ray propagation. For convergence directions at high angles to the dip axis, generally the case at most present-day subduction zones, large dip angles imply strong sampling of the fast axis. In contrast, for flow parallel to the dip axis (e.g., Model DA), the intermediate axis will be primarily sampled in the mantle. Because velocities in the slab (for the same dip) will, in general, be some linear combination of the fast and intermediate axes, Model CD will generally yield negative velocity contrasts and Model DA positive contrasts.

The "guided P phase" will see greater positive velocity contrasts because less of the slow axis is sampled in the subducting lithosphere than for ScSp paths. All models predict positive velocity contrasts for low dip angles and large θ values. Even for these ideal geometries, however, the velocity contrasts are too low for two of the three models, especially when computed with reasonable mantle mineralogies. Only Model DA predicts velocity contrasts comparable to those reported for the Japan Trench.

These results imply that anisotropy can be important in defining the velocity contrast between the overlying mantle and the subducting lithospheric mantle if there is dynamically induced trench-parallel olivine crystal alignment in the overlying mantle. If such alignment does not occur in subduction zones, however, then seismic anisotropy renders more difficult the explanation of observed velocity contrasts.

Acknowledgements This research was supported by the NSF (EAR-9158594 and EAR-902476) and the PRF of the American Chemical Society (25115-G8). We thank Mark Woods, Ray Russo, George Helffrich, Shun Karato, and an anonymous reviewer for many insightful and useful comments.

References

Ando, M., Y. Ishikawa, and F. Yamazaki, Shear wave polarization anisotropy in the upper mantle beneath Honshu, Japan, *J. Geophys. Res., 88*, 5850–5864, 1983.

Cande, S. C., J. L. LaBrecque, R. L. Larson, W. C Pitman, III, X. Golovchenko, and W. E. Haxby, Magnetic Lineations of the World's Ocean Basins, *AAPG Map*, AAPG, Tulsa, 1989.

DeMets, C., R. G. Gordon, D. F. Argus, and S. Stein, Current plate motions, *Geophys. J. Int., 101*, 425–478, 1990.

Estey, L., and B. Douglas, Upper mantle anisotropy: a preliminary model, *J. Geophys. Res., 91*, 11,393–11,406, 1986.

Fischer, K., and X. Yang, Anisotropy in the Kuril-Kamchatcka subduction zone structure, *Geophys Res Lett, 21*, 5–8, 1994.

Forsyth, D. W., The early structural evolution and anisotropy of the oceanic upper mantle, *Geophys. J. R. astron. Soc., 43*, 103–162, 1975.

Fukao, Y., K. Kanjo, and I. Nakamura, Deep seismic zone as an upper mantle reflector of body waves, *Nature, 272*, 606–608, 1978.

Fukao, Y., S. Hori, and M. Ukawa, A seismological constraint on the depth of basalt-eclogite transition in a subducting oceanic crust, *Nature, 303*, 413–415, 1983.

Gahagan, L, C Scotese, J Royer, D Sandwell, J Winn, R Tomlins, M Ross, J Newman, R Muller, C Mayes, L Lawver, and C Heubeck, Tectonic fabric map of the ocean basins from satellite altimetry data, *Tectonophysics, 155*, 1–26, 1988.

Gripp, A. E., and R. G. Gordon, Current plate velocities relative to the hotspots incorporating the NUVEL-1 global plate motion model, *Geophys. Res. Lett., 17*, 1109–1112, 1990.

Helffrich, G., S. Stein, and B. Wood, Subduction zone thermal structure and mineralogy and their relation to seismic wave reflections and conversions at the slab/mantle interface, *J. Geophys. Res., 94*, 753–763, 1989.

Hess, H., Seismic anisotropy of the uppermost mantle under oceans, *Nature, 203*, 629–631, 1964.

Karato, S., On the Lehmann discontinuity, *Geophys. Res. Lett., 19*, 2255–2258, 1992.

Karato, S., Importance of anelasticity in the interpretation of seismic anisotropy, *Geophys Res Lett, 20*, 1623–1626, 1993.

Matsuzawa, T., N. Umino, A. Hasegawa, and A. Tagaki, Upper mantle velocity structure estimated from PS converted waves beneath the northeastern Japan arc, *Geophys. J. R. astron. Soc., 86*, 767–787, 1986.

McKenzie, D., Finite deformation during fluid flow, *Geophys. J. R. astr. Soc., 58*, 689–715, 1979.

Musgrave, M. J. P., *Crystal Acoustics*, 288 pp., Holden-Day, San Francisco, CA, 1970.

Nakanishi, I., K. Suyehiro, and T. Yokota, Regional variations of amplitudes of ScSp phases observed in the Japanese islands, *Geophys. J. R. astron. Soc., 67*, 615–634, 1981.

Nishimura, C., and D. Forsyth, The anisotropic structure of the upper mantle in the Pacific, *Geophys. J. R. astr. Soc., 96*, 203–226, 1989.

Peselnick, L., and A. Nicolas, Seismic anisotropy in an ophiolite peridotite: application to oceanic upper mantle, *J. Geophys. Res., 83*, 1227–1235, 1978.

Raitt, R., G. Shor, G. Morris, and H. Kirk, Mantle anisotropy in the Pacific Ocean, *Tectonophysics, 12*, 173–186, 1971.

Ribe, N. M., Seismic anisotropy and mantle flow, *J. Geophys. Res., 94*, 4213–4223, 1989a.

Ribe, N. M., A continuum theory for lattice preferred orientation, *Geophys. Jour., 97*, 199–207, 1989b.

Ribe, N. M., On the relation between seismic anisotropy and finite strain, *J. Geophys. Res., 97*, 8737–8747, 1992.

Ribe, N. M., and Y. Yu, A theory for plastic deformation and textural evolution of olivine polycrystals, *J. Geophys. Res., 96*, 8325–8335, 1991.

Russo, R.M., and P.G. Silver, Trench-parallel flow beneath the Nazca plate from seismic anisotropy, *Science, 263*, 1105–1111, 1994.

Shearer, P. M., and J. A. Orcutt, Compressional and shear wave anisotropy in the oceanic lithosphere - the Ngendei seismic refraction experiment, *Geophys. J. R. astron. Soc., 87*, 967–1003, 1986.

Snoke, J. A., I. S. Sacks, and H. Okada, Determination of subducting lithosphere boundary by use of converted phases, *Bull. Seismol. Soc. Am., 67*, 1051–1060, 1977.

T. Shoberg and C. R. Bina, Department of Geological Sciences, Northwestern University, Evanston, IL 60208-2150.

(Received Dec. 20, 1993; accepted Jan. 13, 1994.)